IEEE Transactions on Nuclear Science, Vol.NS-22, No.3, June 1975

BEAM DYNAMICS EXPERIMENTS IN THE PS BOOSTER

J. Gareyte, L. Magnani, F. Pedersen, F. Sacherer and K. Schindl
CERN, Geneva, Switzerland

Summary

The main problems encountered on the way to 10^{13} ppp have been emittance blow-up and coherent instabilities. The observations and counter measures are described in the text.

Introduction

As described previously[1], the Booster is a slow cycling accelerator composed of four separate, superposed rings, each with 1/4 the PS circumference. Protons from the 50 MeV linac are multiturn injected into each of the four rings, accelerated in five bunches per ring to 800 MeV, and then transferred sequentially into the 20 waiting PS buckets for further acceleration. The space-charge limit in the PS should therefore be raised by the factor 8.3 due to the change in $\beta\gamma^2$, assuming that the normalized emittances are unchanged. With the same emittances, the space-charge limit at 50 MeV in the Booster should be about six times larger than the observed 2×10^{12} ppp limit at 50 MeV in the PS: a factor 4 arises because four rings are used[2], and an additional 1.5 because the Booster bunches are 50% longer than the PS bunches.

After considerable effort spread over a two year period, the best performance obtained so far is the acceleration of a beam with intensity over 10^{13} ppp and with normalized emittances containing 95% of the particles of vertical 19π and horizontal 44π compared with the linac value $10\pi \times 10^{-6}$ rad·m. The peak intensity so far accelerated is 1.4×10^{13}, but with larger emittances. On the other hand, by reducing the number of turns injected, a round beam is obtained with final emittances equal to the linac value and with intensity 5×10^{12} ppp.

Multiturn injection

This works as expected. With the 100 μs linac pulse, up to 15 turns can be injected into each ring. The horizontal normalized emittance is limited to 44π mm·mrad (about half the acceptance) in order to fit through the extraction and transfer channels and into the PS. The performance is summarized in Table 1 for two intensities (the linac pre-buncher is used only for high intensity operation).

Table 1: PSB Multiturn injection performance (1 ring)

Parameter	Intermediate intensity	High intensity
Linac beam current I_L (mA)	50	80
Normalized emittance (π mm·mrad)	8–10	9–12
Number of turns	15	12
Protons at injection point N_L	6.5×10^{12}	9.0×10^{12}
Protons injected N_I	2.4×10^{12}	3.5×10^{12}
Horizontal emittance after injection (π mm·mrad)	44	44
Multiturn efficiency = N_I/N_L		
– achieved	37	39
– computer	43	45

The achieved efficiencies of 35 to 40% agree reasonably well with those obtained from numerical simulation[3], or from approximate formulae.[4]

Adiabatic trapping

This also works very well. For low intensities, 95 to 100% of the injected particles are trapped, while for high intensities the efficiency is between 80 and 85%. Two debunchers in the injection line allow the linac energy spread to be varied over the range ±60 keV to ±450 keV. Best results are obtained with ±150 keV: larger energy spreads exceed the bucket area, while smaller values lead to residual bunch-shape oscillations, and to severe longitudinal instabilities later in the cycle (discussed later). The RF voltage is normally programmed to rise adiabatically from its resting value of 1 kV to its final value of 12 kV in 0.5 ms, and the resulting bunch formation process is shown in Fig. 1 for 3.2×10^{12} particles trapped per ring. At these intensities, space charge reduces the bucket area by about 20%; the final bunch area after trapping is around 7.5 mrad (in units of $\Delta\beta\gamma\cdot\Delta\phi$) or 0.12 electronvolt seconds. A non-adiabatic voltage program has also been experimented with.[5]

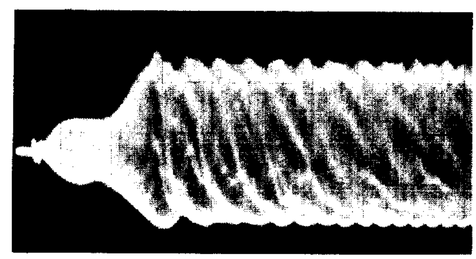

Fig. 1 Σ signal during trapping: 0.2 ms/div.

At high intensities, a beam-loading instability occurs during the voltage rise while the voltage is still low. This is cured by momentarily increasing the dissipation in the power tube, thus lowering the Q of the cavity.[6]

Emittance blow-up

This was always a serious worry[7], especially because of the slow acceleration rate, the emittance ratio of 1 to 4, and the emittance limitation imposed by the subsequent injection into the PS. Figure 2 shows a typical early measurement of the emittance growth along the cycle.

Eventually we realized that most of the blow-up could be explained by repeated stopband crossing due to a combination of synchrotron motion and Laslett Q-shift: since the Q-depression varies along the bunch length from a maximum at the centre to zero at either end, a particle's Q-value is modulated at twice the synchrotron frequency. The area swept out by particles in the Q-diagram is shown in Fig. 3 for typical parameters. The Q-shifts are computed for a beam whose transverse cross-section has a parabolic density distribution[8], and as a result, the Q-shift is about 50%

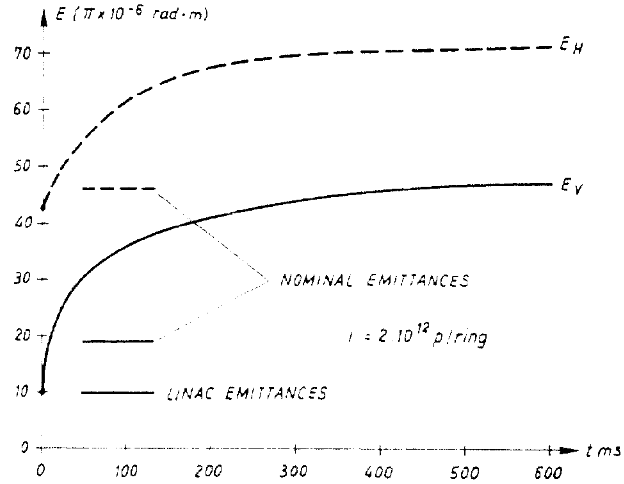

Fig. 2 Emittance growth for point near A of Fig. 3

larger than that given by Laslett's formula (which assumes a uniform density), and has an amplitude dependent octupole term which gives the diagram its width.

If stopbands fall within the shaded area, multiple crossings occur at the rate of 8 to 10 kHz early in the cycle. Typical times observed for doubling the emittance are a few ms for 2nd order stopbands, 50 ms for 3rd order stopbands, and 200 ms or more for 4th order stopbands. Thus point A in Fig. 3 results in a continuous blow-up (the Q-shift decreases by a factor 7 during acceleration), while the blow-up for point B slows down after about 100 ms.

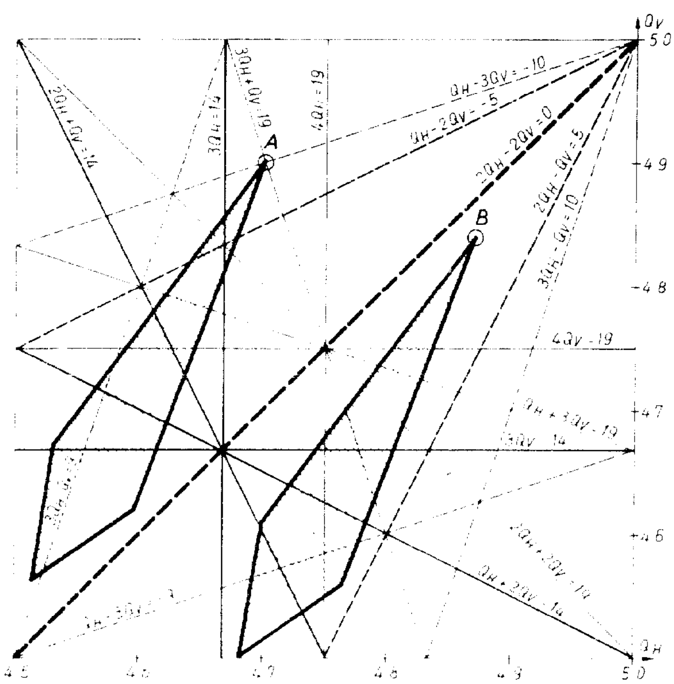

Fig. 3 Area occupied in Q-diagram for $I = 2.5 \times 10^{12}$ protons/ring, bunching factor 0.5, and normalized emittances 10π vertical and 44π horizontal

However, with the denser beams of point B, strong transverse coherent instabilities occur.[9] These are due to wall resistance, and are particularly serious for Q-values just below integers. They can be cured by powering the zero-harmonic octupole lenses, but this unfortunately widens the nearby stopbands and causes further emittance blow-up: the non-zero closed orbit in the lenses leads to a widening of the 3rd order stopbands, while small differences in strength from lense to lense widen the 4th order stopbands. In addition, one must move away from the main diagonal since the coupling resonance $2Q_H - 2Q_V = 0$ is driven directly by the zero-harmonic octupoles. This resonance is also driven by the octupole component of the space-charge force.[10]

Stopband widths have been measured by using some of the compensation lenses: the Q-values are adjusted to overlap a given stopband, and its width is deduced from the compensation current required to prevent emittance blow-up. This is usually done on a low-energy magnetic flat-top using a beam with normal emittances but reduced intensity. The results are compared in Table 2 with the values calculated from field maps of the individual bending magnets and quadrupoles.

Table 2: Some stopband half-widths ΔQ_e with (2) and without (1) zero-harmonic octupoles. A stopband width $\geq 0.5 \times 10^{-4}$ gives noticeable effect over the acceleration cycle.

	2nd order ($2Q_V = 9$)	3rd order ($3Q_V = 14$)		4th order ($2Q_H + 2Q_V = 19$)	
		(1)	(2)	(1)	(2)
Calculated	0.5×10^{-2}	1.5×10^{-4}	$\sim 3 \times 10^{-4}$	2.3×10^{-4}	$2\text{-}6 \times 10^{-4}$
Measured	0.8×10^{-2}	1.6×10^{-4}	2.7×10^{-4}	0.6×10^{-4}	4.0×10^{-4}

A more favourable working region has been used for the past year (Fig. 4): by splitting Q_H and Q_V by an integer, one avoids the strong 4th order coupling resonance $2Q_H - 2Q_V = 0$, and by going just above integers, one reduces the e-folding rate of transverse instabilities. This region is limited above by the strong 3rd order systematic resonance $3Q_V = 16$ (the periodicity of the machine is 16), and by the integer line below. The available area is too small to accommodate the beam considered in Fig. 3, and it immediately blows up, doubling the vertical emittance in a few ms, until it

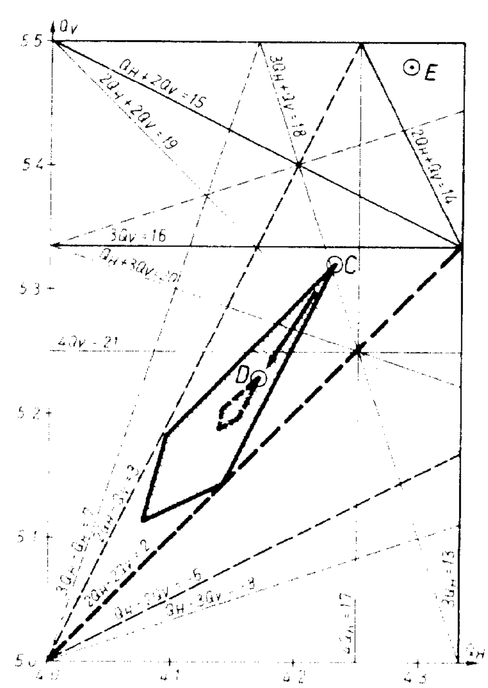

Fig. 4 New working point

fits within the area shown in Fig. 4. Then provided the working point is programmed from C to D during the first 100 ms of acceleration to keep away from the strong sextupolar and weak octupolar stopbands, no further blow-up occurs. A beam with the nominal characteristics can be accelerated in this way (10^{13} ppp in 19π mm•mrad vertical and 44π horizontal). Moreover, a beam with half nominal intensity can be accelerated with no blow-up at all (5×10^{12} ppp in 10π mm•mrad vertical and horizontal). For the future, additional correcting lenses have been ordered, and should allow the working regions to be enlarged.

Longitudinal instabilities

Centre-of-mass motion of the individual bunches develops within a few ms after trapping (Fig. 5) and grows slowly until by the end of the cycle the bunches are often moving by more than one bunch length (Fig. 6). The phase relationship between different bunches appears to be random and changes along the cycle, so this is not the usual coupled-bunch instability. The threshold depends strongly on linac energy spread, or equivalently, bunch length: one gains a factor of five in current by increasing the energy spread from ±90 keV (210 ns bunches) to ±150 keV (250 ns bunches), which is the optimum value. Still larger energy spreads reduce the trapping efficiency. Without special cures, at most 0.8×10^{13} can be accelerated in the four rings.

Two cures have been tried. The first is to reduce the RF voltage until the bucket just fits the bunch, thus increasing the frequency spread within the bunch. However the spread is concentrated at the bunch edge, and the centre continues to oscillate. In addition, with the reduced voltage a beam-loading instability of the Robinson type occurs, but complicated by AVC, phase and tuning loops.[11]

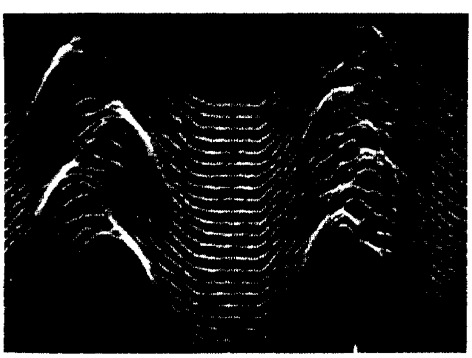

Fig. 5 Centre-of-mass motion developing after trapping

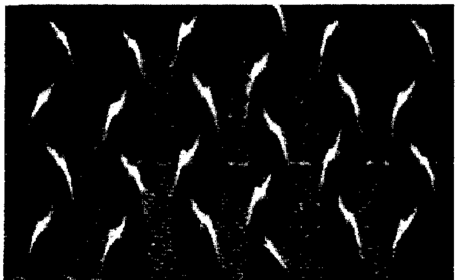

Fig. 6 Bunch motion at end of cycle

The cure now used is to modulate the RF frequency with a constant signal near 4.2 kHz. During acceleration, the synchrotron frequency varies from 5 to 2 kHz, and therefore is swept through the applied "shaking" frequency just after trapping. This rearranges the particles within the bunch, lowering the peak density by about 1/3, and increasing the bunch length by a few per cent. The effect on the instability is dramatic, as the before and after traces in Fig. 7 show.

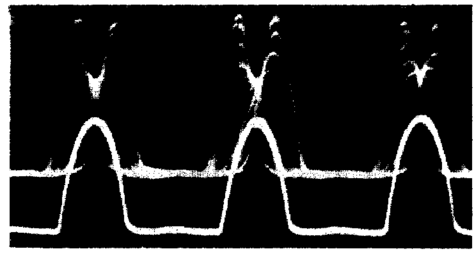

Fig. 7

The best results are obtained when the frequency crossing occurs just after trapping, and the amplitude is set near to the loss level (modulation of about ±4 RF degrees). A second crossing later in the cycle when the bucket is larger is used to remove any remaining oscillations and to increase the bunch length from 55 ns to about 70 ns, which eases transition crossing and instability problems in the PS. Phase or amplitude modulation at twice the synchrotron frequency is also effective.

With this technique of directly modifying the bunch distribution, intensities well over 10^{13} ppp can be accelerated. However, at the highest intensities, the settings are critical and the "shaking" results in about 5 to 10% losses along the cycle. Ultimately, some combination of this technique with active feedback or voltage reduction may be the best solution.

Discussion

Although the cause of the instability is not known, the strong dependence on bunch length and bunch shape is not surprising. The usual stability criterion is[12]

$$S \gtrsim F\,|\Delta\omega| \tag{1}$$

where S is the frequency spread within the bunch, $\Delta\omega$ is the frequency shift due to self-forces, and F depends on the particle distribution. For the Booster, the dominant contribution to $\Delta\omega$ is the repulsive space-charge force between protons, which has an L^{-3} dependence, while $S \propto L^2$, and therefore one expects a threshold that depends on the 5th power of bunch length. Also, for this case where $\Delta\omega$ is predominantly real, one finds from the dispersion relation that F is proportional to the central density of particles in the synchrotron phase plane, so bunches with lower central density are expected to be more stable. The magnitudes are also about right.

The shaking technique has also been used to measure the incoherent frequencies within the bunch. On a magnetic flat-top, a constant applied frequency can produce a notch in the bunch as shown in Fig. 8. The location of this notch vs applied frequency is plotted in Fig. 9 for two intensities. The frequency shift vs intensity is about right, but the frequencies are lower than expected. The coherent frequency is also plotted, and one sees that it falls outside the bunch spectrum. This is the condition for instability, and is equivalent to criterion (1).

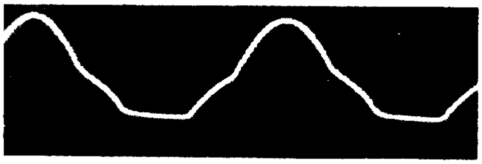

Fig. 8

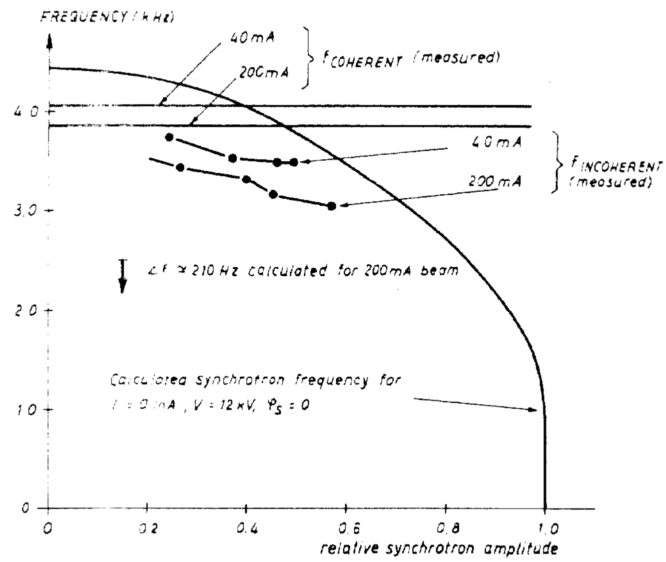

Fig. 9

The absence of coupled-bunch motion during acceleration is also not surprising. The RF sweeps from 3 to 8 MHz so that a resonant element cannot maintain synchronism with the bunches for long, except near the end of the cycle where the sweep slows down. In fact, a coupled-bunch mode has been seen there. Figure 10 shows the bunch frequency spectrum from $5f_0$ to $10f_0$ ($5f_0$ is the RF frequency) during the last 1/3 of the cycle, and one sees a growth at frequencies $7f_0$ and $8f_0$. In fact, only the lower synchrotron sideband of $7f_0$ and the upper of $8f_0$ are growing. The sidebands expected for coupled-bunch mode n, with phase-shift $n \times 72°$ between adjacent bunches, are shown in Fig. 11; so mode n = 3 is being excited. According to theory, a resonator must overlap one of the lower sidebands (below transition energy) to cause instability, so we expect a resonance near $2f_0$, $7f_0$, $12f_0$, or $17f_0$. At higher frequencies, the quadrupole or breathing mode would be excited. The cause of this instability has not been found yet.

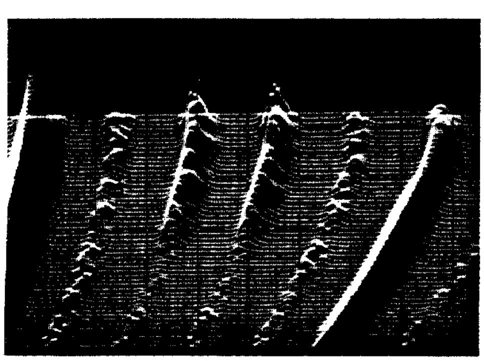

Fig. 10 Bunch frequency spectrum

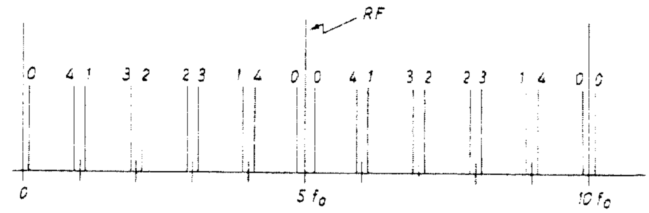

Fig. 11

We have also seen a pure sextupole mode (Fig. 12); this oscillates at three times the synchrotron frequency and has no centre-of-mass or breathing component.

Fig. 12 Sextupole mode

References

1) C. Bovet et al., Proc. 1973 Particle Accelerator Conf., IEEE Trans. Nuclear Sci. NS-20, 221 (1973).
2) W. Hardt, Proc. 5th Int. Conf. on High-Energy Accelerators (Frascati, 1965), p. 151.
3) C. Bovet et al., Proc. 8th Int. Conf. on High-Energy Accelerators (Geneva, 1971), p. 102.
4) K. Schindl, P. van der Stok, CERN/MPS/BR Int./74-2 (1974).
5) I. Gumowski, D. Zanaschi, Bunch shape oscillation control in RF trapping, this conference.
6) G. Gelato et al., Evolution of the RF system of the CPS booster since the beginning of the operation, this conference.
7) C. Bovet et al., Proc. 8th Int. Conf. on High-Energy Accelerators (Geneva, 1971), p. 380.
8) H. Schönauer, private communication.
9) J. Gareyte, F. Sacherer, Proc. 9th Int. Conf. on High-Energy Accelerators (Stanford, 1974), p. 341.
10) E.W. Montague, Fourth-order coupling resonance excited by space-charge forces in a synchrotron, CERN 68-38 (1968).
11) F. Pedersen, Beam loading effects in the CERN PS booster, this conference.
12) F. Sacherer, Proc. 1973 Particle Accelerator Conf., IEEE Trans. Nuclear Sci. NS-20, 825 (1973).

Acknowledgement

This work would not have been possible without the strong support of the Booster Operations and Systems teams.